

# BLOCKWISE SFT FOR DIFFUSION LANGUAGE MODELS: RECONCILING BIDIRECTIONAL ATTENTION AND AUTOREGRESSIVE DECODING

Bowen Sun<sup>1</sup> Yujun Cai<sup>2\*</sup> Ming-Hsuan Yang<sup>1,3</sup> Yiwei Wang<sup>1</sup>

<sup>1</sup>University of California, Merced <sup>2</sup>The University of Queensland <sup>3</sup>Google DeepMind

sunbowen0728@gmail.com

<https://github.com/Bowen-Sun-0728/Blockwise-SFT>

## ABSTRACT

Discrete diffusion language models have shown strong potential for text generation, yet standard supervised fine-tuning (SFT) misaligns with their semi-autoregressive inference: training randomly masks tokens across the entire response, while inference generates fixed-size blocks sequentially. This mismatch introduces noisy prefixes and leaky suffixes, biasing gradients away from the desired blockwise likelihood. We propose *Blockwise SFT*, which partitions responses into fixed-size blocks, selects one active block per step for stochastic masking, freezes all preceding tokens, and fully hides future ones. Loss is computed only over the active block, directly mirroring the blockwise decoding process. Experiments on GSM8K (Cobbe et al., 2021), MATH (Hendrycks et al., 2021), and MetaMathQA (Yu et al., 2024) show consistent gains over classical SFT under equal compute or token budgets. Block size consistency studies and ablations confirm that improvements stem from faithful training–inference alignment rather than incidental masking effects. Our results highlight the importance of matching supervision granularity to the decoding procedure in diffusion-based language models.

## 1 INTRODUCTION

Large language models based on discrete diffusion have moved from proofs of concept to competitive conditional generators (Gong et al., 2023). Intuitively, a diffusion LM learns to undo noise: during training it corrupts response tokens with a relaxed categorical process and predicts the clean tokens; during inference it starts from noise and iteratively denoises over multiple steps to produce text. In parallel, semi-autoregressive decoding has emerged as a practical middle ground between fully parallel refinement and strict left-to-right generation: systems such as SSD-LM (Han et al., 2023) generate fixed-size blocks sequentially, exploiting within-block parallelism while preserving cross-block causality. Modern dLLMs, including the LLaDA family (Nie et al., 2025), expose blockwise inference as a first-class interface. This setting raises a simple question that motivates our work: *can a training objective based on bidirectional attention and full-sequence random masking serve a model that will be decoded causally, block by block?*

The prevailing supervised fine-tuning (SFT) recipe for diffusion LMs is misaligned with that use case. Classical SFT randomly masks tokens across the entire response and reconstructs them in a single pass. At inference, the model instead receives a clean, deterministic prefix and produces exactly one block while the future is fully hidden. As illustrated in Figure 1, this mismatch produces three concrete issues: (i) *noisy prefixes*—training conditions on corrupted contexts that never appear at test time; (ii) *dependency leakage*—training may reveal tokens inside or beyond the target block, violating the causal structure required at inference; and (iii) a *granularity mismatch*—loss is computed token by token while decisions at inference are made block by block.

We introduce *Blockwise SFT* to close this gap. The idea is to make training look like deployment. At each step, we focus learning on a single *active block*. The prefix before it is kept clean and frozen,

---

\*Corresponding author.

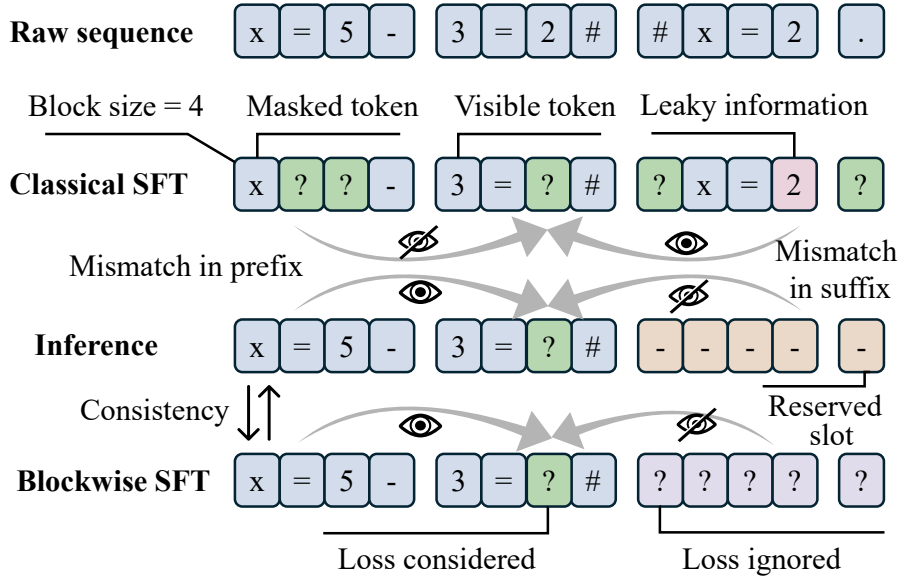


Figure 1: Classical SFT, Blockwise SFT, and autoregressive inference.

the suffix after it is fully hidden, and the loss is computed only on the active block. This alignment preserves cross-block causality, concentrates supervision where the next decision is made, and is architecture-agnostic: any diffusion LM that decodes in blocks can adopt it without changing its network or sampler.

The contributions of this work encompass three key aspects. We first diagnose why full-response SFT is ill-suited for semi-autoregressive, blockwise decoding in discrete diffusion LMs, showing that random masking creates *noisy prefixes* and *dependency leakage* (Figure 1). We then introduce *Blockwise SFT*, a drop-in objective that supervises one active block given a clean prefix and a hidden future, requiring no architectural changes or exotic schedules. Finally, we provide theory explaining when and why this alignment works: the objective forms a variational upper bound on blockwise likelihoods, simple block/time sampling yields unbiased gradient estimates, and the gradient bias of classical SFT under mismatch can be characterized precisely (see §3.3).

In short, aligning the training signal with the decoding procedure matters. Blockwise SFT turns a widely adopted inference pattern into an equally principled training objective, yielding models that are both more accurate and more efficient to fine-tune. We validate this claim by fine-tuning on MetaMathQA and evaluating on GSM8K and MATH, observing consistent gains under matched compute and matched supervision budgets, improved early-training efficiency, and state-of-the-art results in a head-to-head comparison (Table 1). Analyses further show that accuracy peaks when training and inference use the same block size (§4.5) and degrades with injected prefix noise or suffix visibility (§4.6).

## 2 RELATED WORK

**Discrete Diffusion Models for Text Generation** Diffusion has been extended to discrete text via Argmax Flows and Multinomial Diffusion (Hoogeboom et al., 2021), which map tokens to continuous space and add categorical noise during training. D3PMs (Austin et al., 2023) generalize this with structured corruption processes to better capture token relationships. DiffuSeq (Gong et al., 2023) applies diffusion to conditional sequence-to-sequence tasks, matching or surpassing autoregressive baselines. Recent evaluations (Weligalle, 2025) highlight trade-offs between modeling quality and generation speed.

**Supervised Fine-Tuning Methods** For autoregressive LLMs, SFT trains on cross-entropy loss over response tokens (Ouyang et al., 2022), with variants such as instruction tuning (Wei et al., 2023;

Chung et al., 2022) improving generalization. Diffusion-based LLMs use iterative refinement, with SFT approaches (Austin et al., 2023; Li et al., 2022) reconstructing randomly masked tokens in one step. This departs from the blockwise, semi-autoregressive decoding common in diffusion models, creating a training–inference mismatch.

**Autoregressive Decoding in Diffusion-Based Language Models** Early discrete diffusion generators were slow and sometimes incoherent. SSD-LM (Han et al., 2023) introduced semi-autoregressive decoding: generating fixed-size blocks with diffusion denoising while freezing prior blocks. Block Diffusion (Arriola et al., 2025) interpolates between pure diffusion and fully autoregressive sampling via block decomposition and KV-caching, improving flexibility and throughput. Adaptive Parallel Decoding (APD) (Israel et al., 2025) adjusts block size by uncertainty, combining diffusion marginals with an autoregressive verifier to approach AR speeds with minimal quality loss.

**Contemporary diffusion–SFT variants.** Beyond classical SFT, several recent variants target efficiency or stability rather than decoding alignment. **MDLM** introduces a simplified, substitution-based objective that reduces to a mixture of masked-LM losses and, with a strong training recipe, narrows the gap to autoregressive models (Sahoo et al., 2024). **Soft-Masked Diffusion LM** replaces hard corruption with linguistically informed soft-masking and applies per-step cross-entropy to better handle discrete tokens and reduce cost (Chen et al., 2023). **RDM** reparameterizes discrete diffusion, producing alternative training and sampling procedures that improve text generation quality (Zheng et al., 2024). **Two-Step Loss & Scheduling** explicitly mitigates train–inference discrepancy by training with a two-step diffusion and gradually increasing self-conditioning probability (Asada & Miwa, 2025). These approaches primarily refine the diffusion objective, noise schedule, or parameterization while continuing to supervise randomly across the whole response. In contrast, our *Blockwise SFT* aligns the granularity of supervision with semi-autoregressive, blockwise decoding (clean prefix, hidden future, loss on the active block). Under equal compute budget, this alignment yields consistent gains over all above variants on GSM8K and MATH (Table 1).

### 3 METHODOLOGY

#### 3.1 OVERVIEW AND INTUITION.

Classical SFT teaches a diffusion LM to fill in randomly masked tokens anywhere in the response, using bidirectional attention over whatever remains visible. Deployment looks different: semi-autoregressive decoding commits one block at a time, conditioning on a clean prefix and never peeking at future tokens. Imagine a short math line “ $x = 5 - 3 = ?$ ”. Training might corrupt the “5” or even show the answer token; inference never sees either event—it always receives an untouched prefix and must decide the next block causally.

Our remedy is to make training look like deployment. At each step we choose the *active block*—the next contiguous chunk the model would emit—keep the prefix exactly as it will appear at inference, fully hide the suffix, and place the loss only on the active block. The rest of this section turns this story into equations, states the three guarantees we rely on (one variational bound and two properties of the stochastic estimator), and defers proofs and estimator details to the appendix.

#### 3.2 CLASSICAL SUPERVISED FINE-TUNING FOR DISCRETE DIFFUSION AND ITS LIMITATIONS

**Method recap.** Given an instruction–response sequence  $\mathbf{x}_{1:L} = [\mathbf{c}; \mathbf{r}]$ , Classical SFT draws a binary mask  $\mathbf{m}_{1:L}$  over *response* tokens, independently per token with probability  $\pi$ :

$$m_i \sim \text{Bernoulli}(\pi), \quad i \in \{L_c + 1, \dots, L\}.$$

Let  $\tilde{\mathbf{x}} = \mathbf{x} \odot (1 - \mathbf{m})$  be the masked input. With  $T$  diffusion steps, forward kernel  $q_t(\mathbf{z}_t \mid \mathbf{x})$ , reverse model  $\mathbf{p}_\theta(\mathbf{x} \mid \mathbf{z}_t, t)$ , and weights  $\{\omega_t\}_{t=1}^T$ , the loss is

$$\mathcal{L}_{\text{SFT}}(\theta) = \sum_{t=1}^T \omega_t \mathbb{E}_{\mathbf{x}, \mathbf{m}, \mathbf{z}_t} \left[ - \sum_{i=1}^L \mathbf{1}[m_i = 1] \log p_\theta(x_i \mid \mathbf{z}_t, t) \right], \quad (1)$$

i.e., an MLM-style cross-entropy at each diffusion step. Intuitively, the model learns to undo noise: training recovers clean tokens from a noised input; inference starts from noise and denoises iteratively to produce text.

**Limitations under blockwise decoding.** Blockwise decoding commits decisions one block at a time. Let  $B$  be the block size; index the next-to-generate block by  $a$ ; write its token indices as  $\mathcal{I}_a$ ; and let  $\mathcal{I}_{\text{prefix}}^{(a)} / \mathcal{I}_{\text{suffix}}^{(a)}$  be indices before / after block  $a$ . Relative to the blockwise risk in equation 3 (defined below), Classical SFT creates three specific mismatches:

(i) *Prefix corruption.* Training corrupts the conditioning context with probability

$$\Pr[\exists i \in \mathcal{I}_{\text{prefix}}^{(a)} : m_i = 1] = 1 - (1 - \pi)^{|\mathcal{I}_{\text{prefix}}^{(a)}|},$$

whereas inference always uses a clean, deterministic prefix.

(ii) *Suffix leakage.* Training can leave future tokens visible with probability

$$\Pr[\exists j \in \mathcal{I}_{\text{suffix}}^{(a)} : m_j = 0] = 1 - \pi^{|\mathcal{I}_{\text{suffix}}^{(a)}|},$$

allowing bidirectional attention to exploit information that will be hidden at deployment.

(iii) *Granularity mismatch.* The loss in equation 1 spreads supervision across all response positions. In expectation, the supervised mass on the active block is  $\pi |\mathcal{I}_a|$ , identical (up to size) to that allocated to non-active blocks. In contrast, decoding cares about the next block, which we formalize next; the dispersion of learning signal leads to the bias quantified by Theorem 3.3.

### 3.3 DERIVING THE BLOCKWISE SFT OBJECTIVE

**From decoding to a training risk.** Write the response  $\mathbf{r}$  as  $M$  consecutive blocks  $\mathbf{b}^{(1)}, \dots, \mathbf{b}^{(M)}$  after the instruction  $\mathbf{c}$ . Under semi-autoregressive decoding, the sequence likelihood factorizes as

$$p_\theta(\mathbf{x}) = \prod_{a=1}^M p_\theta(\mathbf{b}^{(a)} \mid \mathbf{context}^{(a)}, t=0), \quad (2)$$

where  $\mathbf{context}^{(a)} = \mathbf{x}_{1:L_c+B(a-1)}$  is the clean prefix up to block  $a-1$ , and  $\mathbf{b}^{(a)} = \mathbf{x}_{L_c+B(a-1)+1:L_c+Ba}$  are tokens of block  $a$ . The risk we care about is the sum of blockwise NLLs,

$$\mathcal{R}_{\text{block}}(\theta) = \mathbb{E}_{\mathbf{x}} \left[ - \sum_{a=1}^M \log p_\theta(\mathbf{b}^{(a)} \mid \mathbf{context}^{(a)}, t=0) \right], \quad (3)$$

so training should align its gradients with equation 3, not with a full-response denoising objective that mixes prefixes and leaks suffix information.

**A block-local diffusion surrogate.** To match decoding, we select an active block  $a$ , keep the prefix clean (no gradient), fully hide the suffix, and apply diffusion cross-entropy only within  $a$ . Let  $\mathcal{I}_a$  be indices of block  $a$ , and let  $\mathbf{z}_t \sim q_t(\cdot \mid \mathbf{x})$  be the noised state at step  $t$ . Define

$$\tilde{\mathcal{L}}_t(\theta; \mathbf{x}, a) = - \sum_{i \in \mathcal{I}_a} \log p_\theta(x_i \mid \mathbf{z}_t, t), \quad \mathcal{L}_{\text{BW-SFT}}(\theta) = \mathbb{E}_{\mathbf{x}, a} \left[ \sum_{t=1}^T \omega_t \mathbb{E}_{\mathbf{z}_t} [\tilde{\mathcal{L}}_t(\theta; \mathbf{x}, a)] \right]. \quad (4)$$

Single- $t$  sampling and importance weighting that recover the  $t$ -sum in equation 4 are given in Appendix A.5.

**Why this surrogate is faithful.** Applying the discrete-diffusion ELBO *only* to the masked active block—conditioning on the clean prefix and hiding the suffix—yields a variational upper bound on the blockwise NLL.

**Theorem 3.1** (Variational upper bound for blockwise likelihood). *For suitable nonnegative weights  $\{\omega_t\}_{t=1}^T$  and a constant  $C$  independent of  $\theta$ ,*

$$- \log p_\theta(\mathbf{b}^{(a)} \mid \mathbf{context}^{(a)}, t=0) \leq \sum_{t=1}^T \omega_t \mathbb{E}_{\mathbf{z}_t \sim q_t(\cdot \mid \mathbf{x})} [\tilde{\mathcal{L}}_t(\theta; \mathbf{x}, a)] + C, \quad (5)$$

and hence  $\mathcal{R}_{\text{block}}(\theta) \leq \mathcal{L}_{\text{BW-SFT}}(\theta) + C'$  with  $C'$  independent of  $\theta$ . Proof in Appendix A.6.

**Unbiased gradients under block/time sampling.** Sampling the active block and the diffusion step yields an unbiased estimator of the surrogate gradient; appropriate reweighting recovers the full objective.

**Theorem 3.2** (Unbiasedness of blockwise gradients; importance weighting). *Let  $a \sim \rho$  over  $\{1, \dots, M\}$  and  $t \sim \tilde{\omega}$  with  $\tilde{\omega}_t = \omega_t / \sum_{s=1}^T \omega_s$ . Define*

$$\hat{g}(\theta) = \frac{1}{\rho(a)} \left( \sum_{s=1}^T \omega_s \right) \nabla_{\theta} \mathbb{E}_{\mathbf{z}_t \sim q_t(\cdot|\mathbf{x})} [\tilde{\mathcal{L}}_t(\theta; \mathbf{x}, a)].$$

*Then  $\mathbb{E}[\hat{g}(\theta)] = \nabla_{\theta} \mathcal{L}_{\text{BW-SFT}}(\theta)$  for any  $\rho$ . If a local fidelity condition holds,  $\mathbb{E}[\hat{g}(\theta)] = \nabla_{\theta} \mathcal{R}_{\text{block}}(\theta)$  (up to a global scalar). Proof in Appendix A.6.*

**Why classical SFT is biased under mismatch.** Noisy prefixes and leaky suffixes induce a systematic gradient bias when training with Classical SFT but decoding blockwise.

**Theorem 3.3** (Classical SFT gradient bias under mismatch). *Let  $\nabla_{\theta} \ell^*(\theta; \mathbf{x}, a)$  be the clean active-block gradient  $\nabla_{\theta} [-\log p_{\theta}(\mathbf{b}^{(a)} \mid \text{context}^{(a)}, t=0)]$ , and  $\nabla_{\theta} \ell^{\text{cls}}(\theta; \mathbf{x}, a)$  be the Classical-SFT gradient with mask rate  $\pi$ . If the gradient map is  $L_{\text{pre}}$ -Lipschitz w.r.t. prefix perturbations and  $L_{\text{suf}}$ -Lipschitz w.r.t. suffix perturbations (holding the active block fixed), then*

$$\| \mathbb{E}[\nabla_{\theta} \ell^{\text{cls}}(\theta; \mathbf{x}, a)] - \nabla_{\theta} \ell^*(\theta; \mathbf{x}, a) \| \leq L_{\text{pre}} \cdot (1 - (1 - \pi)^{|\mathcal{I}_{\text{prefix}}^{(a)}|}) + L_{\text{suf}} \cdot (1 - \pi^{|\mathcal{I}_{\text{suffix}}^{(a)}|}). \quad (6)$$

Proof in Appendix A.6.

**Takeaways.** The surrogate in equation 4 (i) upper-bounds the blockwise NLL (Theorem 3.1), (ii) admits unbiased stochastic gradients via block/time sampling (Theorem 3.2), and (iii) corrects the gradient bias inherent to Classical SFT under blockwise decoding (Theorem 3.3). This explains why aligning the objective with the decoding procedure is both principled and effective.

### 3.4 PRACTICAL IMPLEMENTATION OF BLOCKWISE SFT

**Objective.** Let  $\mathcal{I}_a$  be the indices of the active block  $a$ . The Blockwise SFT loss is

$$\mathcal{L}_{\text{BW-SFT}}(\theta) = \sum_{t=1}^T \omega_t \mathbb{E}_{\mathbf{x}, a, \mathbf{z}_t} \left[ - \sum_{i \in \mathcal{I}_a} \log p_{\theta}(x_i \mid \mathbf{z}_t, t) \right], \quad (7)$$

with gradients back-propagated only through  $\mathcal{I}_a$ , matching the semi-autoregressive factorization in §3.3.

**Algorithm.** Algorithm 1 gives a single training step for *Blockwise SFT*. In brief: partition the response into fixed-size blocks, sample one *active block*, keep the prefix clean and the suffix hidden, sample a mask rate and a diffusion step, compute the block-local diffusion loss, and update  $\theta$  using gradients from that block only (notation matches §3.3).

## 4 EXPERIMENT

### 4.1 DATASETS AND TASKS

**MetaMathQA.** We train on meta-math/MetaMathQA<sup>1</sup>, a large-scale math QA corpus built from GSM8K and MATH training questions via multiple rewrites, with no test leakage. The commonly used split contains  $\sim 395\text{K}$  examples, each paired with a reference answer.

**Evaluation Sets.** For evaluation, we use the test splits of openai/gsm8k<sup>2</sup> and HuggingFaceH4/MATH-500<sup>3</sup>. GSM8K contains grade-school-level arithmetic word problems, while MATH covers advanced competition-style problems across algebra, geometry, number theory, and combinatorics. We report *Pass@1* accuracy, computed by exact string match between the model’s prediction and the reference answer.

<sup>1</sup><https://huggingface.co/datasets/meta-math/MetaMathQA>

<sup>2</sup><https://huggingface.co/datasets/openai/gsm8k>

<sup>3</sup><https://huggingface.co/datasets/HuggingFaceH4/MATH-500>

---

**Algorithm 1** Blockwise SFT — One Training Step

---

**Require:** Instruction–response pair  $\mathbf{x} = [\mathbf{c}; \mathbf{r}]$ ; block size  $B$ ; diffusion steps  $T$ ; per-step weights  $\{\omega_t\}_{t=1}^T$ ; model  $\theta$ ; forward kernel  $q_t$

- 1: **Partition response** into blocks  $\mathbf{r} = [\mathbf{b}^{(1)}, \dots, \mathbf{b}^{(M)}]$  with index sets  $\{\mathcal{I}_m\}_{m=1}^M$  where  $M = \lceil L_r/B \rceil$
- 2: **Sample active block**  $a \sim \text{Uniform}\{1, \dots, M\}$
- 3: **Sample masking rate**  $\pi \sim \text{Uniform}(0, 1)$
- 4: **Build mask**  $\mathbf{m}_{1:L}$ :
  - Prefix ( $i \leq L_c + B(a-1)$ ):  $m_i \leftarrow 0$  (clean; no gradient)
  - Active block ( $i \in \mathcal{I}_a$ ):  $m_i \leftarrow \text{Bernoulli}(\pi)$
  - Suffix ( $i > L_c + Ba$ ):  $m_i \leftarrow 1$  (fully hidden)
- 5: **Sample diffusion step**  $t$  with probability  $\tilde{\omega}_t = \omega_t / \sum_{s=1}^T \omega_s$  (single- $t$  variant; see App. A.5)
- 6: **Noise** the sequence:  $\mathbf{z}_t \sim q_t(\cdot | \mathbf{x})$
- 7: **Compute block-local loss**  $\tilde{\mathcal{L}}_t(\theta; \mathbf{x}, a) = -\sum_{i \in \mathcal{I}_a} \log p_\theta(x_i | \mathbf{z}_t, t)$
- 8: **Scale by**  $Z = \sum_{s=1}^T \omega_s$  and take gradient of  $Z \cdot \mathbb{E}_{\mathbf{z}_t}[\tilde{\mathcal{L}}_t]$  (unbiased for equation 7)
- 9: **Backpropagate** only through positions  $i \in \mathcal{I}_a$ ; treat prefix as constants and suffix as masked
- 10: **Update**  $\theta$  with AdamW and the shared hyperparameters (App. A.1)

---

#### 4.2 BASELINES AND COMPARISONS

**Models.** We compare three configurations: Base (no supervision), Classical SFT (randomly mask the full response each step), and Blockwise SFT (mask only the active block while keeping the prefix clean and the suffix hidden).

**Why two comparison protocols?** The two methods differ in (i) how much compute each update costs and (ii) how many response tokens receive supervision. To make the comparison fair, we report results under two complementary controls: EQUAL-FLOPS (fix compute) and EQUAL-TOKENS (fix supervised-token budget).

**EQUAL-FLOPS.** For diffusion LMs, each training step runs the Transformer over the *entire* sequence at every layer (and diffusion step), so the dominant cost—self-attention and MLP—depends on sequence length, not on which tokens receive loss. Consequently, when optimizer steps, batch size, sequence length, and the number of diffusion steps are fixed, the per-step FLOPs are essentially identical for Classical SFT and Blockwise SFT; masking only changes where the loss (and nonzero gradients) appear, not the forward/backward compute graph. Example: with  $L_r=128$  and  $B=32$  ( $M=4$  blocks), one epoch over  $N$  samples executes the same forward/backward work for both methods; Classical SFT supervises all 128 response tokens, whereas Blockwise SFT supervises only the 32 tokens in the sampled block. In practice, we therefore train both for one epoch on the same  $N$  with identical settings—matching compute while varying where gradients land (see Figure 2).

**EQUAL-TOKENS.** Here we match the total number of supervised response tokens. We define one *traversal* as: on average, each response token is supervised once. Using the same example ( $L_r=128$ ,  $B=32$ ), after one epoch Classical SFT achieves one traversal (all 128 tokens supervised), while Blockwise SFT achieves 1/4 traversal (only one 32-token block). To compare at one traversal, we run Classical SFT for 1 epoch and Blockwise SFT for 4 epochs, sampling different blocks over time. This protocol fixes the supervised-token budget and isolates how supervision is distributed across blocks; compute is not constrained.

**Implementation details.** We fine-tune all models with LoRA (Hu et al., 2021). We adopt the hyperparameters of Biderman et al. (2024) verbatim, because LoRA is sensitive to optimizer and adapter settings and exposes many coupled knobs; exhaustive search is costly and unnecessary for our purpose. We scale the learning rate with the square-root rule (Krizhevsky, 2014).

For both methods, the Bernoulli masking rate is sampled as  $\pi \sim \text{Uniform}(10^{-3}, 1)$  at the sequence (Classical SFT) or active-block (Blockwise SFT) level, following the fine-tuning recipe of LLaDA (Nie et al., 2025). After applying the Bernoulli mask, if no position is masked in the supervision region, we additionally mask the last token of that region—i.e., the last token of the full response for Classical SFT, or the last token of the active block for Blockwise SFT.

Experiments use GSAI-ML/LLaDA-8B-Instruct<sup>4</sup>. All runs use a single NVIDIA A100 (80 GB). With identical dataloader and optimizer settings, both methods reach  $\sim 5.1\text{k tokens s}^{-1}$ . We train in bfloat16 (Micikevicius et al., 2018) using AdamW (Loshchilov & Hutter, 2019) with linear warm-up and cosine decay (Smith, 2017). Full hyperparameters appear in Appendix A.1. With per-device batch size 1, peak usage is  $\approx 23.5$  GB, so all experiments are feasible on a 24 GB consumer GPU (e.g., RTX 3090) or any device with comparable or larger memory.

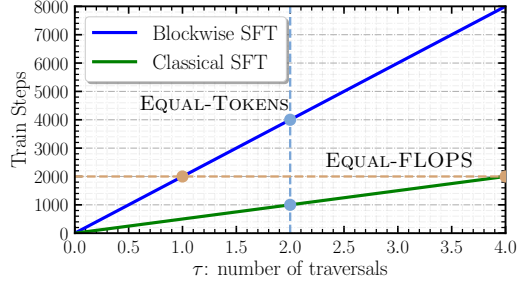


Figure 2: EQUAL-FLOPS vs. EQUAL-TOKENS.

### 4.3 MAIN RESULTS

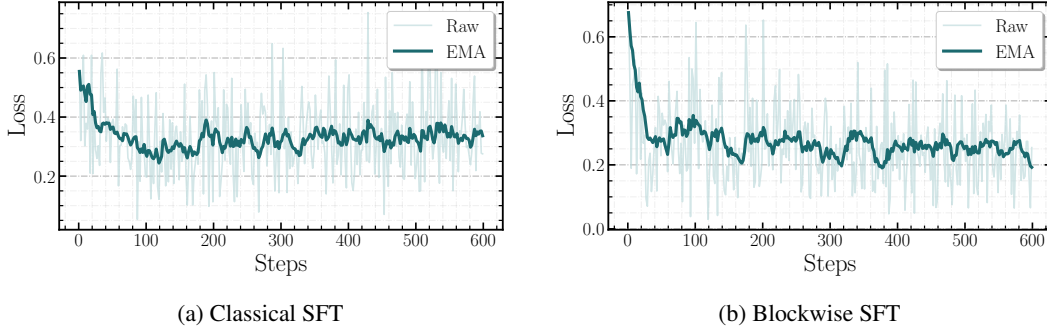


Figure 3: Loss as a function of training steps.

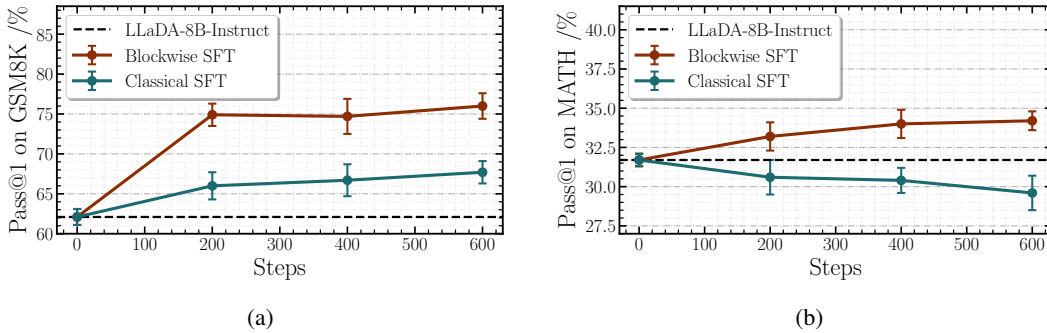


Figure 4: Performance as a function of training steps under EQUAL-FLOPS.

<sup>4</sup><https://huggingface.co/GSAI-ML/LLaDA-8B-Instruct>

**Results under EQUAL-FLOPS.** Figure 3 first presents the training loss. Both methods show a rapid drop in the first 50–100 steps, after which the exponential-moving-average (EMA) curves flatten. Near convergence the short-term oscillation amplitudes are similar, but the steady levels differ markedly: Blockwise SFT stabilizes around 0.24 (Figure 3b), whereas Classical SFT stabilizes around 0.36 (Figure 3a).

Figure 4 reports Pass@1 under matched forward–backward token operations (EQUAL-FLOPS) on GSM8K (Figure 4a) and MATH (Figure 4b). On GSM8K, all methods improve sharply within the first 100–200 steps and then slow, but **Blockwise SFT** stays well above **Classical SFT** throughout, reaching  $\approx +10$  Pass@1 at the final checkpoint and consistently exceeding the LLaDA-8B-Instruct baseline. On MATH, **Blockwise SFT** again improves steadily, whereas **Classical SFT** degrades over training and remains below the Base model at every checkpoint. These trends indicate that supervision aligned with semi-autoregressive decoding yields stronger accuracy under fixed compute.

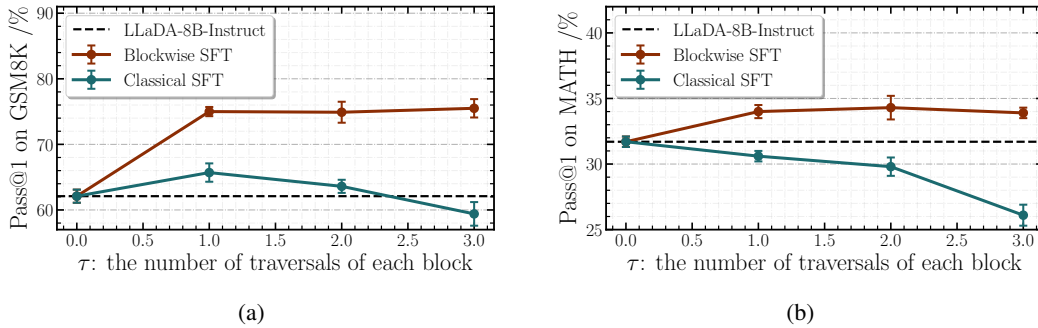


Figure 5: Performance as a function of training steps under EQUAL-TOKENS.

#### Results under EQUAL-TOKENS.

Figure 5 reports Pass@1 as a function of traversal count  $\tau$  under EQUAL-TOKENS (Figure 5a for GSM8K and Figure 5b for MATH; cf. §4.2). Across both datasets, **Blockwise SFT** achieves a substantial gain already at  $\tau = 1$  and then remains comparatively stable as  $\tau$  increases (through  $\tau = 3$ ).

On **GSM8K**, **Classical SFT** shows only a small lift at  $\tau = 1$ , far below Blockwise SFT, and then drops rapidly; by  $\tau = 3$  it underperforms the Base model. On **MATH**, Classical SFT degrades steadily with larger  $\tau$ , typically below the baseline across most traversals, while Blockwise SFT makes modest gains up to  $\tau = 1$  and then stabilizes. These results mirror the EQUAL-FLOPS trends and indicate that block-aligned supervision delivers earlier gains and more stable learning under matched token budgets.

#### 4.4 HEAD-TO-HEAD COMPARISON

We benchmark seven systems under matched compute (EQUAL-FLOPS): the Base model, Classical SFT (D3PM-style masked diffusion (Austin et al., 2023)), four improved SFT variants—MDLM (Sahoo et al., 2024), Soft-Masked Diffusion LM (Chen et al., 2023), RDM (Zheng et al., 2024), and Two-Step Loss & Scheduling (Asada & Miwa, 2025)—and our Blockwise SFT. All models are fine-tuned on MetaMathQA with identical tokenization, optimization, and decoding settings; only the supervision mechanism differs. As summarized in Table 1, Blockwise SFT attains the best Pass@1 on both benchmarks (GSM8K:  $76.0 \pm 1.6$ ; MATH:  $34.2 \pm 0.5$ ). Relative to the strongest non-Blockwise baseline (Two-Step Loss & Scheduling,  $70.8 \pm 1.3$  /  $32.6 \pm 0.7$ ), the gains are +5.2 points on GSM8K and +1.6 on MATH. On MATH, Classical SFT trails the Base model ( $29.6 \pm 0.7$  vs.  $31.7 \pm 0.4$ ), while recent variants offer only modest improvements (e.g., RDM  $32.3 \pm 0.6$ , Two-Step  $32.6 \pm 0.7$ ). On GSM8K, several variants exceed Classical SFT (e.g., MDLM  $68.4 \pm 1.9$ ), but none approach Blockwise SFT. Overall, the head-to-head results under matched compute substantiate the superiority of Blockwise SFT over 4 other enhanced algorithms derived from Classical SFT.



Table 1: Head-to-head comparison under EQUAL-FLOPS: Pass@1 (%) on GSM8K and MATH.

Method	GSM8K (Pass@1)	MATH (Pass@1)
<b>Base (no FT)</b>	$62.1 \pm 1.0$	$31.7 \pm 0.4$
<b>Classical SFT</b> (Austin et al., 2023)	$67.7 \pm 1.4$	$29.6 \pm 0.7$
MDLM (Sahoo et al., 2024)	$68.4 \pm 1.9$	$31.9 \pm 0.5$
Soft-Masked Diffusion LM (Chen et al., 2023)	$67.7 \pm 0.8$	$29.9 \pm 0.6$
RDM (Zheng et al., 2024)	$65.5 \pm 1.5$	$32.3 \pm 0.6$
Two-Step Loss & Scheduling (Asada & Miwa, 2025)	$70.8 \pm 1.3$	$32.6 \pm 0.7$
<b>Blockwise SFT (Ours)</b>	<b><math>76.0 \pm 1.6</math></b>	<b><math>34.2 \pm 0.5</math></b>

#### 4.5 BLOCK SIZE CONSISTENCY STUDY

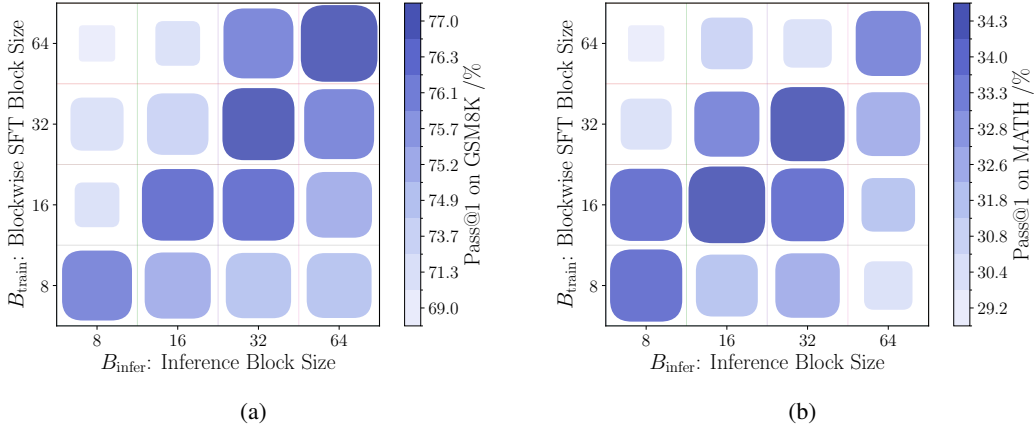


Figure 6: Combinations of Blockwise SFT training block size  $B_{\text{train}}$  and inference block size  $B_{\text{infer}}$ .

We train two  $4 \times 4$  grids over  $B_{\text{train}}, B_{\text{infer}} \in \{8, 16, 32, 64\}$  to measure sensitivity to block-size mismatch. As shown in Figure 6, accuracy is highest on the diagonal ( $B_{\text{train}} = B_{\text{infer}}$ ) and remains strong for near-diagonal pairs (small  $|B_{\text{train}} - B_{\text{infer}}|$ ), while it degrades markedly as combinations move farther off the diagonal (e.g.,  $8 \rightarrow 64$  or  $64 \rightarrow 8$ ). Across both heatmaps, the diagonal and its immediate neighbors form the best-performing band, indicating that Blockwise SFT’s gains are primarily driven by aligning training with the semi-autoregressive decoding granularity rather than any particular block size.

#### 4.6 ABLATION EXPERIMENTS

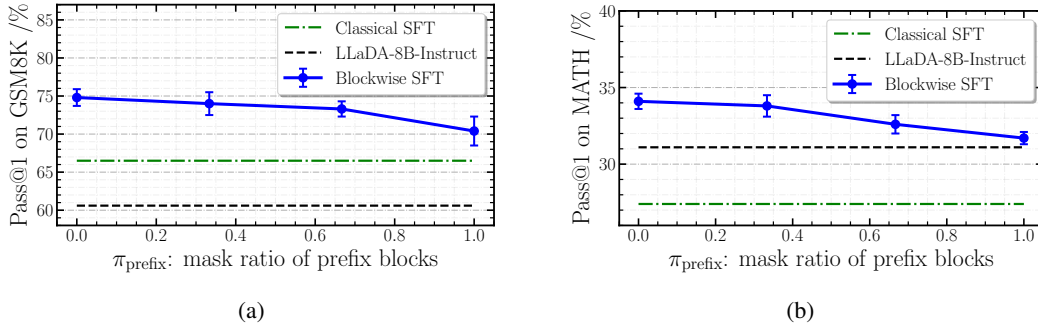


Figure 7: Performance as a function of  $\pi_{\text{prefix}}$ .

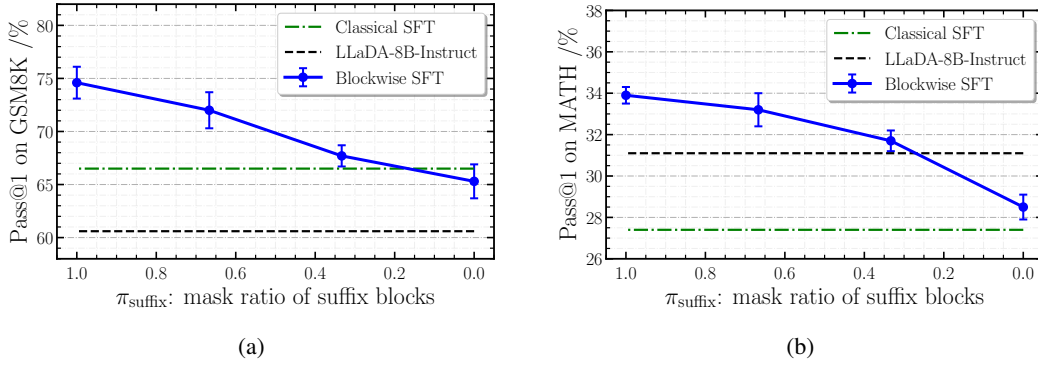


Figure 8: Performance as a function of  $\pi_{\text{suffix}}$ .

**Prefix noise** ( $\pi_{\text{prefix}}$ , mask ratio over prefix blocks). In Figure 7, a small mask rate (e.g.,  $\pi_{\text{prefix}}=0.33$ ) causes only minor loss on both GSM8K and MATH, but accuracy degrades markedly as  $\pi_{\text{prefix}}$  increases, with the largest drop at  $\pi_{\text{prefix}}=1.0$ . This pattern matches the mechanism: prefix masking corrupts the conditioning context except when the active block is the first (no prefix to mask), so  $\pi_{\text{prefix}}=1$  behaves like a reduction in the fraction of instances that contribute gradients—some samples remain unaffected—but the frequent noisy contexts still hurt performance. Overall, the ablation confirms that controlling prefix contamination is a key factor for Blockwise SFT, consistent with the need for a clean, deterministic prefix at inference.

**Suffix leakage** ( $\pi_{\text{suffix}}$ , mask ratio over suffix blocks). In Figure 8, performance drops clearly as  $\pi_{\text{suffix}}$  decreases (i.e., as more future tokens become visible). When  $\pi_{\text{suffix}} = 0$  (fully visible suffix), the scores approach those of Classical SFT on both datasets, indicating that strict future masking is the key factor behind Blockwise SFT’s advantage. Implementation details for both ablations are provided in Appendix A.7.

## 5 CONCLUSION

We introduced *Blockwise SFT*, a simple fine-tuning strategy that aligns supervision with semi-autoregressive, blockwise decoding in discrete diffusion LMs. By freezing clean prefixes, masking only the active block, and strictly hiding future tokens, Blockwise SFT removes the contextual shift and dependency leakage inherent to classical SFT. The objective is theoretically grounded—providing a variational upper bound on blockwise likelihoods, admitting unbiased block/time-sampled gradients, and explaining the bias of classical SFT under mismatch (Theorems 3.1–3.3). Empirically, fine-tuning on MetaMathQA with evaluation on GSM8K and MATH yields consistent gains under matched compute and token budgets, state-of-the-art results in a head-to-head comparison, and diagnostic trends that track training–inference alignment (block-size consistency in §4.5, prefix/suffix ablations in §4.6).

Beyond accuracy, the recipe is easy to adopt—no architectural changes, a drop-in loss, and practical single-step estimators (§3.4). Limitations and avenues for future work include adaptive or uncertainty-aware block sizing, combining blockwise supervision with preference/RL-style objectives for instruction following, and extending the alignment principle to other semi- or non-autoregressive generators. Overall, respecting the structural constraints of the decoding procedure is not just an efficiency tweak but a core ingredient for performance in diffusion-based language models.

## REFERENCES

Marianne Arriola, Aaron Gokaslan, Justin T. Chiu, Zhihan Yang, Zhixuan Qi, Jiaqi Han, Subham Sekhar Sahoo, and Volodymyr Kuleshov. Block diffusion: Interpolating between autoregressive and diffusion language models, 2025. URL <https://arxiv.org/abs/2503.09573>.

- Masaki Asada and Makoto Miwa. Addressing the training-inference discrepancy in discrete diffusion for text generation. In Owen Rambow, Leo Wanner, Marianna Apidianaki, Hend Al-Khalifa, Barbara Di Eugenio, and Steven Schockaert (eds.), *Proceedings of the 31st International Conference on Computational Linguistics*, pp. 7156–7164, Abu Dhabi, UAE, January 2025. Association for Computational Linguistics. URL <https://aclanthology.org/2025.coling-main.477/>.
- Jacob Austin, Daniel D. Johnson, Jonathan Ho, Daniel Tarlow, and Rianne van den Berg. Structured denoising diffusion models in discrete state-spaces, 2023. URL <https://arxiv.org/abs/2107.03006>.
- Dan Biderman, Jacob Portes, Jose Javier Gonzalez Ortiz, Mansheej Paul, Philip Greengard, Connor Jennings, Daniel King, Sam Havens, Vitaliy Chiley, Jonathan Frankle, Cody Blakeney, and John P. Cunningham. Lora learns less and forgets less, 2024. URL <https://arxiv.org/abs/2405.09673>.
- Jiaao Chen, Aston Zhang, Mu Li, Alex Smola, and Diyi Yang. A cheaper and better diffusion language model with soft-masked noise, 2023. URL <https://arxiv.org/abs/2304.04746>.
- Hyung Won Chung, Le Hou, Shayne Longpre, Barret Zoph, Yi Tay, William Fedus, Yunxuan Li, Xuezhi Wang, Mostafa Dehghani, Siddhartha Brahma, Albert Webson, Shixiang Shane Gu, Zhuyun Dai, Mirac Suzgun, Xinyun Chen, Aakanksha Chowdhery, Alex Castro-Ros, Marie Pellat, Kevin Robinson, Dasha Valter, Sharan Narang, Gaurav Mishra, Adams Yu, Vincent Zhao, Yanping Huang, Andrew Dai, Hongkun Yu, Slav Petrov, Ed H. Chi, Jeff Dean, Jacob Devlin, Adam Roberts, Denny Zhou, Quoc V. Le, and Jason Wei. Scaling instruction-finetuned language models, 2022. URL <https://arxiv.org/abs/2210.11416>.
- Karl Cobbe, Vineet Kosaraju, Mohammad Bavarian, Mark Chen, Heewoo Jun, Lukasz Kaiser, Matthias Plappert, Jerry Tworek, Jacob Hilton, Reiichiro Nakano, Christopher Hesse, and John Schulman. Training verifiers to solve math word problems, 2021. URL <https://arxiv.org/abs/2110.14168>.
- Shansan Gong, Mukai Li, Jiangtao Feng, Zhiyong Wu, and Lingpeng Kong. Diffuseq: Sequence to sequence text generation with diffusion models, 2023. URL <https://arxiv.org/abs/2210.08933>.
- Xiaochuang Han, Sachin Kumar, and Yulia Tsvetkov. Ssd-lm: Semi-autoregressive simplex-based diffusion language model for text generation and modular control, 2023. URL <https://arxiv.org/abs/2210.17432>.
- Dan Hendrycks, Collin Burns, Saurav Kadavath, Akul Arora, Steven Basart, Eric Tang, Dawn Song, and Jacob Steinhardt. Measuring mathematical problem solving with the math dataset, 2021. URL <https://arxiv.org/abs/2103.03874>.
- Emiel Hooeboom, Didrik Nielsen, Priyank Jaini, Patrick Forré, and Max Welling. Argmax flows and multinomial diffusion: Learning categorical distributions, 2021. URL <https://arxiv.org/abs/2102.05379>.
- Edward J. Hu, Yelong Shen, Phillip Wallis, Zeyuan Allen-Zhu, Yanzhi Li, Shean Wang, Lu Wang, and Weizhu Chen. Lora: Low-rank adaptation of large language models, 2021. URL <https://arxiv.org/abs/2106.09685>.
- Daniel Israel, Guy Van den Broeck, and Aditya Grover. Accelerating diffusion llms via adaptive parallel decoding, 2025. URL <https://arxiv.org/abs/2506.00413>.
- Alex Krizhevsky. One weird trick for parallelizing convolutional neural networks, 2014. URL <https://arxiv.org/abs/1404.5997>.
- Xiang Lisa Li, John Thickstun, Ishaan Gulrajani, Percy Liang, and Tatsunori B. Hashimoto. Diffusion-lm improves controllable text generation, 2022. URL <https://arxiv.org/abs/2205.14217>.

- Ilya Loshchilov and Frank Hutter. Decoupled weight decay regularization, 2019. URL <https://arxiv.org/abs/1711.05101>.
- Paulius Micikevicius, Sharan Narang, Jonah Alben, Gregory Diamos, Erich Elsen, David Garcia, Boris Ginsburg, Michael Houston, Oleksii Kuchaiev, Ganesh Venkatesh, and Hao Wu. Mixed precision training, 2018. URL <https://arxiv.org/abs/1710.03740>.
- Shen Nie, Fengqi Zhu, Zebin You, Xiaolu Zhang, Jingyang Ou, Jun Hu, Jun Zhou, Yankai Lin, Ji-Rong Wen, and Chongxuan Li. Large language diffusion models, 2025. URL <https://arxiv.org/abs/2502.09992>.
- Long Ouyang, Jeff Wu, Xu Jiang, Diogo Almeida, Carroll L. Wainwright, Pamela Mishkin, Chong Zhang, Sandhini Agarwal, Katarina Slama, Alex Ray, John Schulman, Jacob Hilton, Fraser Kelton, Luke Miller, Maddie Simens, Amanda Askell, Peter Welinder, Paul Christiano, Jan Leike, and Ryan Lowe. Training language models to follow instructions with human feedback, 2022. URL <https://arxiv.org/abs/2203.02155>.
- Subham Sekhar Sahoo, Marianne Arriola, Yair Schiff, Aaron Gokaslan, Edgar Marroquin, Justin T Chiu, Alexander Rush, and Volodymyr Kuleshov. Simple and effective masked diffusion language models, 2024. URL <https://arxiv.org/abs/2406.07524>.
- Leslie N. Smith. Cyclical learning rates for training neural networks, 2017. URL <https://arxiv.org/abs/1506.01186>.
- Jason Wei, Xuezhi Wang, Dale Schuurmans, Maarten Bosma, Brian Ichter, Fei Xia, Ed Chi, Quoc Le, and Denny Zhou. Chain-of-thought prompting elicits reasoning in large language models, 2023. URL <https://arxiv.org/abs/2201.11903>.
- Ashen Weligalle. Discrete diffusion models for language generation, 2025. URL <https://arxiv.org/abs/2507.07050>.
- Longhui Yu, Weisen Jiang, Han Shi, Jincheng Yu, Zhengying Liu, Yu Zhang, James T. Kwok, Zhenguo Li, Adrian Weller, and Weiyang Liu. Metamath: Bootstrap your own mathematical questions for large language models, 2024. URL <https://arxiv.org/abs/2309.12284>.
- Lin Zheng, Jianbo Yuan, Lei Yu, and Lingpeng Kong. A reparameterized discrete diffusion model for text generation, 2024. URL <https://arxiv.org/abs/2302.05737>.

## A APPENDIX

### A.1 FULL HYPERPARAMETER SETTINGS

Table 2 lists the full hyperparameter configuration used in all experiments reported in the main paper. Unless otherwise specified, parameters not listed (e.g., weight decay, gradient clipping) are set to their default values. The configuration is kept identical across all experimental protocols (EQUAL-FLOPS, EQUAL-TOKENS) and other studies to ensure fair comparison.

### A.2 DATASET PREPROCESSING AND EVALUATION PROTOCOLS

**Training Set.** We follow the preprocessing instructions provided by the MetaMathQA dataset. For each sample, the query field is inserted into the following instruction template:

Below is an instruction that describes a task.  
Write a response that appropriately completes the request.

### Instruction:  
{instruction}

### Response: Let’s think step by step.

Table 2: hyperparameter configuration for all experiments.

Category	Parameter	Value / Description
<b>Batch Size</b>	Number of GPUs	1
	Per-device batch size	32
	Gradient accumulation steps	1
	Global batch size	32
<b>Learning Rate Schedule</b>	Learning rate	$1 \times 10^{-5}$
	Scheduler type	Warmup + Cosine decay
	Warmup steps	10% of total steps
	Cosine decay minimum ratio	0.1
<b>Masking</b>	Mask ratio $\pi$	Uniform( $10^{-3}$ , 1) sampled per sequence / active block
<b>Optimizer (AdamW)</b>	$\beta_1$	0.95
	$\beta_2$	0.99
	Weight decay	0
<b>LoRA</b>	Rank $r$	256
	$\alpha$	512
	Dropout	0.05
	Target modules	Attention and MLP layers
	Bias	None

The placeholder `{instruction}` is replaced with the actual query text. We then concatenate this instruction with the `response` field using the model’s chat template to form the final training sequence. To reduce compute and facilitate reproducibility, the maximum sequence length is set to 256 tokens; samples exceeding this limit (fewer than 10% of the dataset) are discarded. The MetaMathQA dataset contains no samples from the GSM8K or MATH test sets.

**Test Sets.** For evaluation, we apply the same instruction template to the prompts from the test splits of GSM8K and MATH(MATH-500), ensuring identical formatting between training and evaluation inputs.

**Scoring Rules.** We report Pass@1 accuracy for both datasets using exact match:

- **GSM8K:** We extract the *last* numeric value from the model output (e.g., using a regex that matches the final signed/decimal number) and perform exact string match against the reference answer.
- **MATH:** No extraction or normalization is applied because of the complexity of the answer format; we compare the full model output to the reference answer by exact string match.

### A.3 DETAILED INFERENCE SETTINGS

Table 3 summarises the inference-time configurations used throughout our experiments, including both the default settings and the variations for the Block Size Consistency Study. Unless otherwise noted, all other parameters follow the default configuration of the LLaDA-8B-Instruct model.

### A.4 ADDITIONAL PRELIMINARIES AND NOTATION

**Tokenisation and sequences.** Let  $\mathcal{V}$  be a finite vocabulary of size  $V$ . A tokenised sequence is  $\mathbf{x}_{1:L} \in \mathcal{V}^L$  with  $x_i \in \mathcal{V}$ . Each training instance is

$$\mathbf{x}_{1:L} = [\mathbf{c}_{1:L_c}; \mathbf{r}_{1:L_r}], \quad L = L_c + L_r.$$

**Masking operators.** Let  $\mathbf{m}_{1:L} \in \{0,1\}^L$  with  $m_i=0$  for observed and  $m_i=1$  for masked. For **Classical SFT** we sample i.i.d. masks on all response positions:  $m_i \sim \text{Bernoulli}(\pi)$  for

Table 3: Inference-time settings for all experiments.

Parameter	Value / Range	Description
Maximum new tokens	128	Maximum number of tokens generated per example.
Block size	{8, 16, 32, 64} 8 32 (default)	Block Size Consistency Study. Ablation experiments. Default for all other experiments.
Diffusion steps	128 (default)	Number of denoising steps during inference.
Other parameters	Default (LLaDA-8B-Instruct)	All remaining inference parameters follow the model’s official default configuration.

$i \in \{L_c+1, \dots, L\}$ . For **Blockwise SFT**, with active block index  $a$  and block size  $B$ ,

$$m_i = \begin{cases} 0, & i \leq L_c + B(a-1) \quad (\text{prefix}), \\ \text{Bernoulli}(\pi), & L_c + B(a-1) < i \leq L_c + Ba \quad (\text{active block}), \\ 1, & i > L_c + Ba \quad (\text{suffix}). \end{cases}$$

We use  $\tilde{\mathbf{x}} = \mathbf{x} \odot (1 - \mathbf{m})$  to denote the masked sequence. (For variants used in ablations, see Eq. equation 9 in Appendix A.7.)

**Discrete diffusion objective.** Let  $t \in \{0, \dots, T\}$  index diffusion steps and  $q_t(\mathbf{z}_t \mid \mathbf{x})$  be the forward noising kernel (relaxed categorical diffusion). The reverse model  $\mathbf{p}_\theta(\mathbf{x} \mid \mathbf{z}_t, t)$  predicts the original tokens at masked positions. The per-step cross-entropy and the weighted objective are

$$\mathcal{L}_t(\theta) = \mathbb{E}_{\mathbf{x}, \mathbf{m}, \mathbf{z}_t} [\text{CE}(\mathbf{p}_\theta(\cdot \mid \mathbf{z}_t, t), \mathbf{x}) \mid \mathbf{m}], \quad \sum_{t=1}^T \omega_t \mathcal{L}_t(\theta),$$

where  $\{\omega_t\}_{t=1}^T$  are nonnegative weights.

**Notation table.** See Table 4.

Symbol	Meaning
$\mathcal{V}, V$	Vocabulary and its size
$\mathbf{x}_{1:L}$	Full instruction–response sequence
$L_c, L_r$	Instruction and response lengths
$B, M$	Block size and number of response blocks
$a$	Index of the active block
$\mathbf{m}_{1:L}$	Binary mask (1 = latent, 0 = observed)
$T, t$	Total diffusion steps and current step
$q_t, \mathbf{p}_\theta$	Forward kernel and reverse model
$\pi$	Masking rate (sequence or active-block level)

Table 4: Complete notation used in the paper.

## A.5 PRACTICAL ESTIMATORS AND WEIGHTING

**Single- $t$  sampling.** To reduce cost, we may sample a single diffusion step  $t$  with probability  $\tilde{\omega}_t \propto \omega_t$  and multiply the per-step gradient by the normalizer  $Z = \sum_{s=1}^T \omega_s$ . This recovers an unbiased estimate of the  $t$ -sum in equation 4. Formally, letting

$$\hat{\mathcal{L}}(\theta; \mathbf{x}, a, t) = Z \mathbb{E}_{\mathbf{z}_t \sim q_t(\cdot \mid \mathbf{x})} [\tilde{\mathcal{L}}_t(\theta; \mathbf{x}, a)] \quad \text{with } t \sim \tilde{\omega},$$

we have  $\nabla_\theta \mathbb{E}_{t \sim \tilde{\omega}} [\hat{\mathcal{L}}(\theta; \mathbf{x}, a, t)] = \nabla_\theta \sum_{t=1}^T \omega_t \mathbb{E}_{\mathbf{z}_t} [\tilde{\mathcal{L}}_t(\theta; \mathbf{x}, a)]$ .

**Block sampling and importance weights.** If the active block is drawn from a non-uniform distribution  $\rho(a)$ , multiply the per-example gradient by  $1/\rho(a)$  to obtain an unbiased estimator of the block-averaged objective (cf. Theorem 3.2).

## A.6 PROOFS FOR SECTION 3.3

*Proof of Theorem 3.1.* Consider the joint over  $(\mathbf{b}^{(a)}, \{\mathbf{z}_t\}_{t=1}^T)$  under the forward noising process  $q_t(\cdot | \mathbf{x})$  restricted to indices  $\mathcal{I}_a$ , conditioning on  $\mathbf{context}^{(a)}$  and deterministically masking tokens outside  $\mathcal{I}_a$  (suffix). The discrete-diffusion ELBO applied to this restricted chain gives

$$-\log p_\theta(\mathbf{b}^{(a)} | \mathbf{context}^{(a)}) \leq \sum_{t=1}^T \mathbb{E}_{q_t} \left[ \text{KL}(q(\mathbf{z}_{t-1} | \mathbf{z}_t, \mathbf{b}^{(a)}) \| p_\theta(\mathbf{z}_{t-1} | \mathbf{z}_t, \mathbf{context}^{(a)})) \right. \\ \left. - \log p_\theta(\mathbf{b}^{(a)} | \mathbf{z}_1, \mathbf{context}^{(a)}) \right] + C. \quad (8)$$

Standard manipulations for discrete diffusion convert the KL reconstruction terms into tokenwise cross-entropies on  $\mathcal{I}_a$ , producing a weighted sum  $\sum_t \omega_t \mathbb{E}_{q_t} [\tilde{\mathcal{L}}_t(\theta; \mathbf{x}, a)]$ ;  $C$  and the weights depend only on the forward process and are independent of  $\theta$ . Taking expectation over data and summing across  $a$  yields  $\mathcal{R}_{\text{block}}(\theta) \leq \mathcal{L}_{\text{BW-SFT}}(\theta) + C'$  with  $C'$  independent of  $\theta$ .  $\square$

*Proof of Theorem 3.2.* Taking total expectation over  $a \sim \rho$  and  $t \sim \tilde{\omega}$  and using linearity of  $\nabla_\theta$ ,

$$\mathbb{E}[\hat{g}(\theta)] = \sum_{a=1}^M \rho(a) \frac{1}{\rho(a)} \sum_{t=1}^T \tilde{\omega}_t \left( \sum_{s=1}^T \omega_s \right) \nabla_\theta \mathbb{E}_{\mathbf{z}_t} [\tilde{\mathcal{L}}_t(\theta; \mathbf{x}, a)] = \nabla_\theta \mathbb{E}_{\mathbf{x}, a} \sum_{t=1}^T \omega_t \mathbb{E}_{\mathbf{z}_t} [\tilde{\mathcal{L}}_t(\theta; \mathbf{x}, a)],$$

which equals  $\nabla_\theta \mathcal{L}_{\text{BW-SFT}}(\theta)$ . Under Assumption 1 (local surrogate fidelity), replace the inner gradient by that of the  $t=0$  blockwise NLL to obtain  $\nabla_\theta \mathcal{R}_{\text{block}}(\theta)$  up to a global scalar.  $\square$

*Proof of Theorem 3.3.* Express the classical-SFT gradient as an expectation over prefix/suffix masking patterns with mask rate  $\pi$ . If the prefix is fully clean and the suffix fully hidden, the two gradients coincide. Otherwise they differ by at most  $L_{\text{pre}}$  for any masked prefix token and by at most  $L_{\text{suf}}$  for any unmasked suffix token by Lipschitzness. The probability that at least one prefix token is masked equals  $1 - (1 - \pi)^{|\mathcal{I}_{\text{prefix}}^{(a)}|}$ ; the probability that at least one suffix token remains unmasked equals  $1 - \pi^{|\mathcal{I}_{\text{suffix}}^{(a)}|}$ . Taking expectation and applying the triangle inequality yields the bound in equation 6; averaging over  $a$  extends the result to the population gradient bias.  $\square$

## A.7 ABLATION IMPLEMENTATION DETAILS

We formalize the two ablation settings (*Noisy Prefix* and *Leaky Suffix*) as direct modifications to the masking rule in Blockwise SFT (§3.4). Recall that in standard Blockwise SFT, the binary mask  $m_i$  for token  $i$  is defined as:

$$m_i = \begin{cases} 0, & i \leq L_c + B(a-1) \quad (\text{prefix}), \\ \text{Bernoulli}(\pi), & L_c + B(a-1) < i \leq L_c + Ba \quad (\text{active block}), \\ 1, & i > L_c + Ba \quad (\text{suffix}), \end{cases} \quad (9)$$

where  $\pi \in (0, 1)$  is the active-block masking rate, fixed for a given sample. Let  $\mathcal{I}_{\text{prefix}} = \{L_c + 1, \dots, L_c + B(a-1)\}$  denote all prefix tokens (after the prompt and before the active block),  $\mathcal{I}_a$  the indices of the active block, and  $\mathcal{I}_{\text{suffix}} = \{L_c + Ba + 1, \dots, L\}$  the suffix tokens.

**1. Noisy Prefix.** Given a fixed  $\pi_{\text{prefix}} \in [0, 1]$  for the entire experiment, the mask  $m_i$  is modified from equation 9 as:

$$m_i = \begin{cases} \text{Bernoulli}(\pi_{\text{prefix}}), & i \in \mathcal{I}_{\text{prefix}}, \\ \text{Bernoulli}(\pi), & i \in \mathcal{I}_a, \\ 1, & i \in \mathcal{I}_{\text{suffix}}, \end{cases}$$

injecting random noise into the prefix tokens and simulating contextual distribution shift.

**2. Leaky Suffix.** Given a fixed  $\pi_{\text{suffix}} \in [0, 1]$  for the entire experiment, the mask  $m_i$  is modified from equation 9 as:

$$m_i = \begin{cases} 0, & i \in \mathcal{I}_{\text{prefix}}, \\ \text{Bernoulli}(\pi), & i \in \mathcal{I}_a, \\ \text{Bernoulli}(\pi_{\text{suffix}}), & i \in \mathcal{I}_{\text{suffix}}, \end{cases}$$

allowing the model to observe a random fraction of future tokens beyond the active block, thus introducing block-level dependency leakage.

In both cases,  $\pi_{\text{prefix}}$  and  $\pi_{\text{suffix}}$  are fixed for the duration of an experiment and applied identically to all training samples.